UNIVERSITÄT KARLSRUHE

Fakultät für Physik
Dr. A. Denig, Prof. Dr. M. Feindt,
Prof. Dr. G. Quast, Dr. W. Wagner
Dr. A. Vest, Dr. J. Wagner

22. December 2005

Computerpraktikum zur Vorlesung Teilchenphysik für Fortgeschrittene

Reconstructing Top Events in CDF Data

1 Introduction

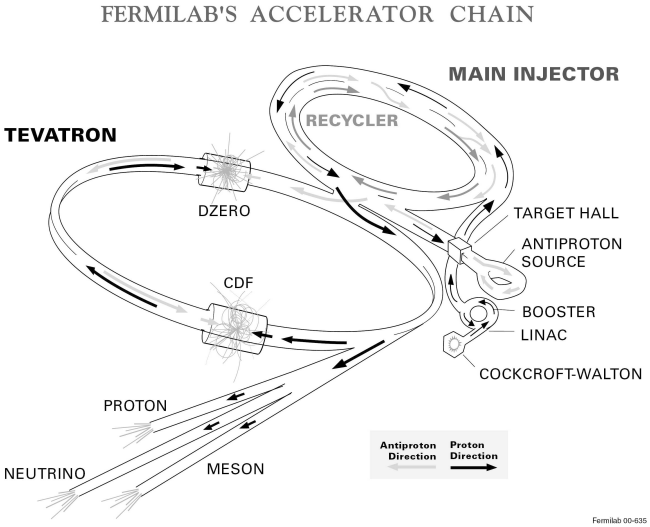

Abbildung 1: *Schematic overview of the TEVATRON accelerator with its two detectors D0 and CDF and its preaccelerators.*

The top quark was discovered by the CDF and D0 collaborations in 1995 at the Tevatron proton anti-proton collider, see figure 1. It still remains one of the least well-studied elementary particles discovered so far. In particular, the measurement of its mass constrains the mass of the Higgs boson, the last particle to be discovered in the Standard Model.

This part of the Computer Praktikum is concerned with the observation of top quarks and with the measurement of the top quark mass. The data used here have been collected from january 2002 till august 2004 by the CDF detector. In the Tevatron ring, intense

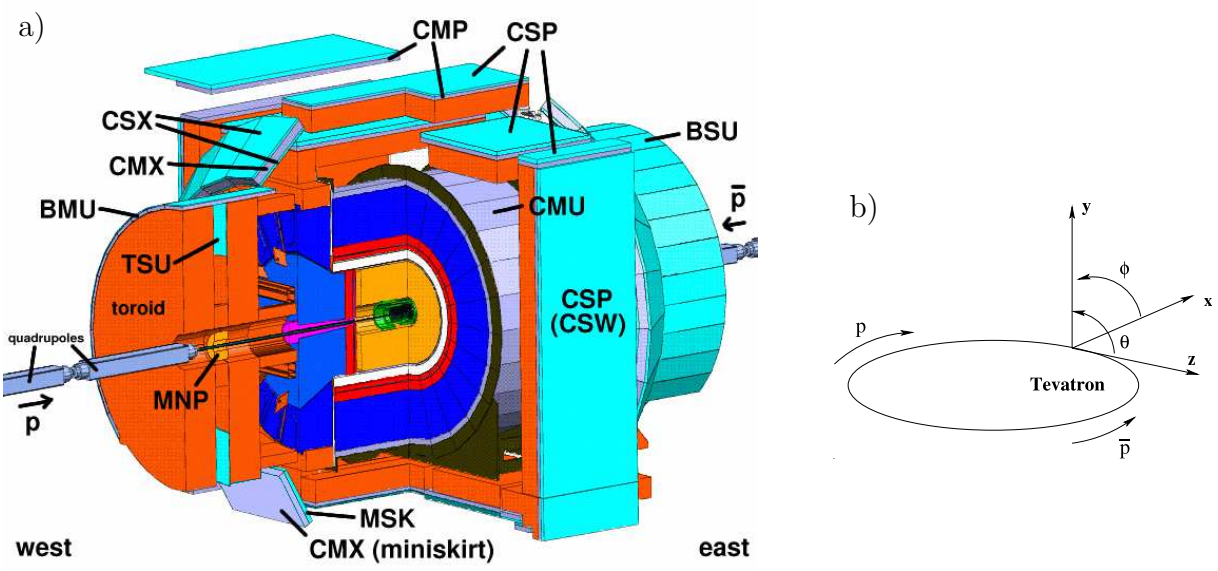

Abbildung 2: a) *Isometric view of the CDF detector in Run II with the abbreviations of the different components of the muon system. The inner green and orange part represents the tracking system and the blue one the calorimeters. b) The coordinate system of the CDF II detector.*

beams of protons and anti-protons are accumulated, accelerated and finally collided in the region of each of the two detectors. The center of mass energy of the proton anti-proton collisions is $\sqrt{s} = 1.96$ TeV.

2 The CDF Detector

The CDF detector is a general purpose detector consisting of several sub detectors for the measurement of the momentum of charged particles (trackers), the energy measurement (calorimeters) and for the muon detection. In figure 2 a) an isometric view of the CDF detector is shown. The right-handed coordinate system used at CDF (fig. 2 b)) has its origin at the nominal interaction point. The z-axis points in the proton beam direction. The x-axis points away from the center of the TEVATRON ring and the y-axis points perpendicular upwards. The azimuthal angle ϕ is given by the angle with the respect to the x-axis in the xy-plane. The polar angle θ is the angle with respect to the z-axis. Thus the polar angle is $\theta = 0°$ in proton direction and $\theta = 180°$ in anti-proton direction. The pseudorapidity is defined by $\eta = -\ln(\tan\frac{\theta}{2})$. A further often used quantity is the rapidity y, which is lorentz invariant except for a constant. The rapidity is defined by $y = 1/2 \cdot \ln((E + p_z)/(E - p_z))$ and is equal to the pseudorapidity for massless objects. E is here the energy and p_z the z-component of the momentum of a particle. The detector components from the inner to the outer are:

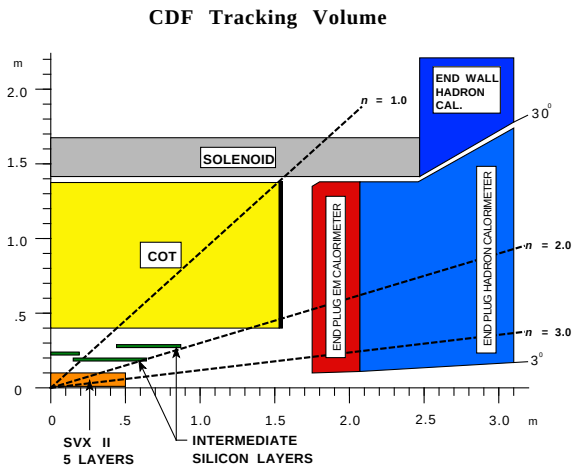

Abbildung 3: *Longitudinal view of the CDF tracking system.*

- **Tracking system**: The Tracking System (figure 3) consists of 3 parts. The SVX, a *Silicon VerteX detector*, the ISL, *Intermediate Silicon Layers* and the COT, the *Central Outer Tracker*, a drift chamber. In the drift chamber the momentum and the direction of charged particles are measured via ionisation in gas, while in the silicon detectors the production of electron-hole pairs is exploited. Closest to the beam pipe is the SVX, which provides a coverage of $|\eta| \leq 2$. The SVX consists of five layers of double sided silicon sensors at radii from 2.4 to 10.7 cm. An impact parameter resolution in ϕ of $< 30\,\mu m$ is achieved for central high momentum tracks. Here, the impact parameter is the distance of closest approach of the track helix to the beam axis measured in the plane perpendicular to the beam. The SVX is followed by the ISL. It consist of one central, forward and backward layer at radii 22 cm and 28 cm respectively. The coverage of the central layer is $|\eta| < 1$ and the coverage of the two outer layer is $1.0 < |\eta| < 2.0$. The purpose of the ISL is to provide enhanced linking of tracks between SVX and COT in the central region. The third part of the tracking system is the COT, a 3.1 m long cylindrical drift chamber, to provide tracking at large radii in the region $|\eta| < 1.0$. The COT covers the radial range from 40 to 137 cm and a hit position resolution of approximately 140 μm and a momentum resolution of $\sigma(p_T)/p_T^2 = 0.0015\,(GeV/c)^{-1}$ is obtained.

- **Super-conducting solenoid**: The tracking system is surrounded by a super-conducting solenoid, 1.5 m in radius and 4.8 m in length, generating a 1.4 T magnetic field parallel to the beam axis.

- **Calorimeter**: The solenoid and tracking volume is surrounded by the calorimeters, designed to measure the energy of particles and jets by fully absorbing all particles except muons and neutrinos. There are, altogether, five calorimeter systems : the CEM,*Central ElectroMagnetic calorimeter*, the CHA, *Central HAdron calorimeter*, the WHA, *end-Wall HAdron calorimeters*, the PEM *end-Plug ElectroMagnetic* and the PHA *end-Plug HAdron calorimeter*, covering 2π in azimuth and in pseudo-

rapidity from $\eta = -3.6$ to $\eta = 3.6$. The purpose of the electromagnetic calorimeters is to measure the energy of electromagnetic showers (caused by e, γ, $\pi^0 \rightarrow \gamma\gamma$), while the hadronic calorimeters are used to measure the energy of the hadronic showers (for example caused by $\pi^{\pm}$, K, n, p, ..). The calorimeters are sampling calorimeters. The active medium is scintillator, the absorber is lead in the electromagnetic calorimeter and iron in the hadronic calorimeter. For this Computer Praktikum only electrons measured in the CEM are used. The coverage of the CEM is $|\eta| < 1.1$ and the energy resolution is $13.5\%/\sqrt{E} \oplus 2\%$.

- **Muon chambers**: Outside of the calorimeter the muon chambers are situated. Four systems of scintillators and drift tubes are used to detect muons at CDF: The *Central MUon Detection System* (CMU), the *Central Muon uPgrade* (CMP), the *Central Muon eXtension* (CMX) and the *Intermediate MUon system* (IMU). The CMU consists of four layers of drift chambers located outside the central hadronic calorimeter which acts as hadron absorber. It covers 84% of the solid angle for the pseudorapidity interval $|\eta| < 0.6$ and could be reached by muons with transverse momenta greater than 1.4 GeV/c. The CMP, which is located behind the CMU, consists of 0.6m of steel and additional four layers of drift chambers behind the steel. For $|\eta| < 0.6$ the CMP covers 63% of the solid angle while both systems have an overlap of 53% of the solid angle. The CMX covers the pseudorapidity range of $0.6 < |\eta| < 1.0$ to 71% of the solid angle and the IMU covers a range from $1.0 < |\eta| < 1.5$. For this Computer Praktikum only muons detected simultaneously in the CMU and CMP are used as well as muons detected in the CMX.

3 Physics of Top Quarks

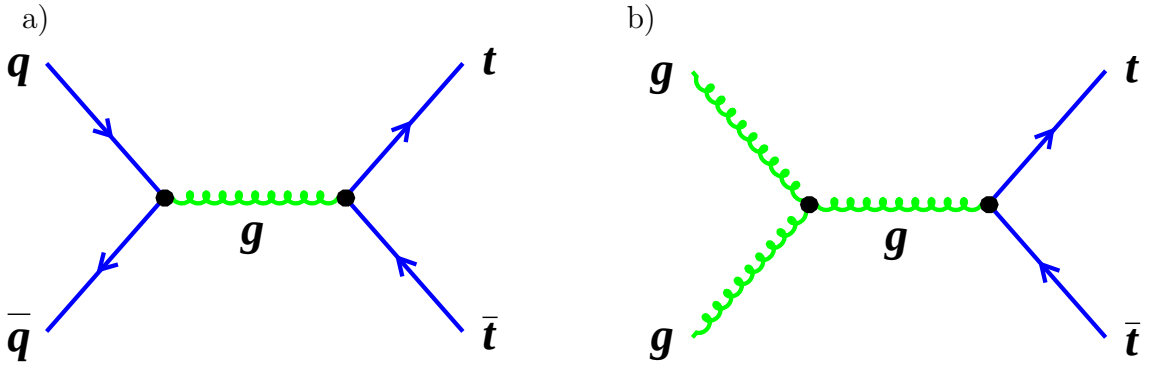

Abbildung 4: *Feynman diagrams of the top anti-top pair production. a) Quark anti-quark annihilation, b) gluon-gluon fusion.*

In $p\bar{p}$ collisions the dominant production mechanism of top quarks is the pair production. The electroweak production of a single top quark is also predicted in the Standard

m_t [GeV]	NLO σ [pb]
170	7.8
175	6.7
180	5.7

Tabelle 1: *$t\bar{t}$ cross section for different top masses as predicted by the NLO calculations from Bonciani et al..*

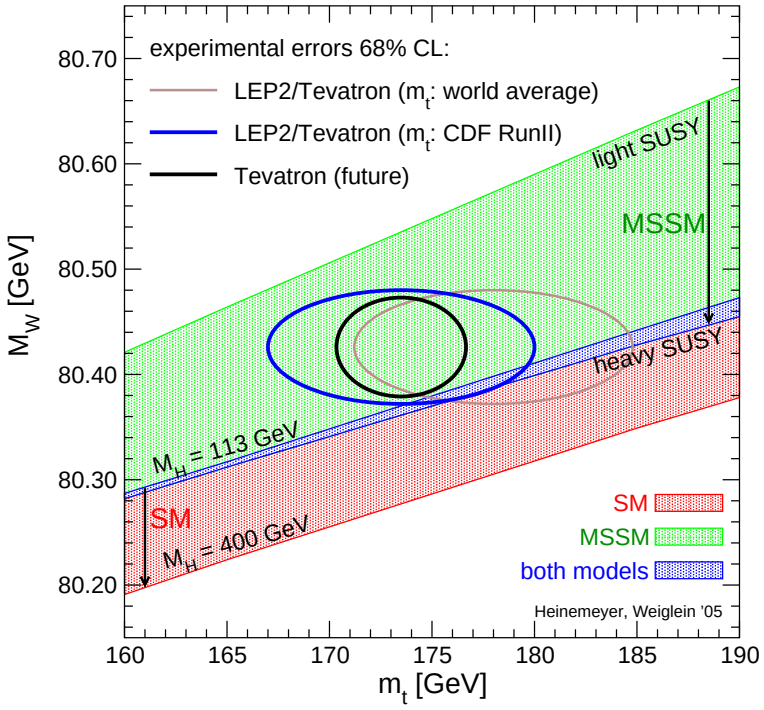

Abbildung 5: *Constraint on the Higgs mass. The W-mass is shown versus the top mass.*

Model. So far no single top was observed. In this Praktikum we look only for $t\bar{t}$-pair production.

At the TEVATRON the top pair is produced through the strong processes quark anti-quark annihilation and gluon-gluon fusion, see figure 4. Here a parton (quark or gluon) of the proton interacts with a parton of the anti-proton. At the Tevatron the quark-antiquark annihilation is with 85% the dominating production mechanism.

Calculations in up to next to leading order (NLO) perturbation theory are available for the $t\bar{t}$ production cross section. The predictions obtained by Bonciani et al. are given in table 1. Since the top quarks are produced at TEVATRON near the threshold, the dependence of the cross section on the top mass is substantial.

The knowledge of the W-boson mass and top quark mass constrains the Higgs mass. That is due to the radiative corrections. Basically, virtual Higgs bosons are continuously

emitted and reabsorbed by top quarks and W bosons, contributing to the observed mass of these particles. But if the top quark is found to be more massive, the Higgs also has to be massive, while the opposite holds for W-bosons. The situation is illustrated in the picture 5. On the x axis is the top quark mass, on the y axis the W boson mass. Each point in this plane with a particular top and W mass is related to a definite value of the as-of-yet unknown Higgs boson mass. There are two bands, the green one shows the theoretically allowed region for an extension of the Standard Model called minimum supersymmetric Standard Model, the red one the allowed region for the Standard Model. Direct measurements of top and W masses are shown by the larger ellipses. The ellipses say, that there is a 68% chance of the two true values of top and W masses to lie within the boundaries. There are different ellipses, corresponding to present and predicted precisions in the measurement of top quark and W boson masses. The blue ellipse, computed with the newest measurement by CDF (spring 2005), speaks in favor of the Supersymmetric extension of the Standard Model, and also advocates a low value for the Higgs boson mass (which increases as the W mass decreases).

4 Signature of Top Antitop Events

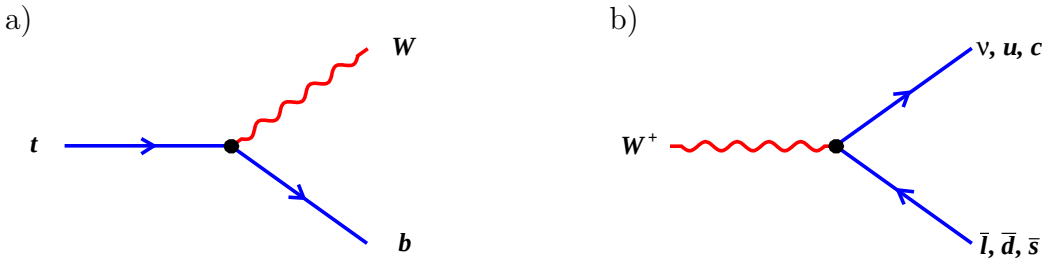

Abbildung 6: *a) Top decay. b) W-decay.*

W decay	Branching ratio
$e^+\nu_e$	$\sim 1/9 = 11.1\%$
$\mu^+\nu_\mu$	$\sim 1/9 = 11.1\%$
$\tau^+\nu_\tau$	$\sim 1/9 = 11.1\%$
$u\bar{d}$	$\sim 3/9 = 33.3\%$
$c\bar{s}$	$\sim 3/9 = 33.3\%$

Tabelle 2: Branching ratio for the W-boson to decay into the various combinations.

The top quark decays with a branching ratio of almost 100% into a b quark and W boson (see figure 6 a)). Due to the strong interaction and the large mass of the top quark

W_1 decay	W_2 decay	Branching ratio
Dilepton channel		
$e^+\nu_e$	$e^+\nu_e$	$\sim 1/81 = 1.2\%$
$e^+\nu_e$	$\mu^+\nu_\mu$	$\sim 2/81 = 2.4\%$
$e^+\nu_e$	$\tau^+\nu_\tau$	$\sim 2/81 = 2.4\%$
$\mu^+\nu_\mu$	$\mu^+\nu_\mu$	$\sim 1/81 = 1.2\%$
$\mu^+\nu_\mu$	$\tau^+\nu_\tau$	$\sim 2/81 = 2.4\%$
$\tau^+\nu_\tau$	$\tau^+\nu_\tau$	$\sim 1/81 = 1.2\%$
Hadronic channel		
$q\bar{q}$	$q\bar{q}$	$\sim 36/81 = 44.4\%$
Lepton + jets channel		
$e^+\nu_e$	$q\bar{q}$	$\sim 12/81 = 14.8\%$
$\mu^+\nu_\mu$	$q\bar{q}$	$\sim 12/81 = 14.8\%$
$\tau^+\nu_\tau$	$q\bar{q}$	$\sim 12/81 = 14.8\%$

Tabelle 3: *Branching ratio of $t\bar{t}$ events for the two W-boson to decay into the various combinations.*

the lifetime of the top quark is with $\tau_t \approx 1/175\ \text{GeV} \cdot (M_W/M_t)^3 = 4.7 \cdot 10^{-25}$ s much smaller than the timescale of the hadronization process $\tau_{QCD} \sim 1/\Lambda_{QCD} \sim 10^{-23}$ s. Thus top quarks decay before they can hadronize. The W-boson itself can decay semileptonically into a lepton and a neutrino or hadronically into quarks, which then hadronize into hadrons. The decay of the W-boson is shown in figure 6 b), while the branching ratios for the different decay modes of the W-boson are summarized in table 2. The two decay possibilities of the W-boson lead to three different event topologies for the reconstruction of $t\bar{t}$ events: the dilepton events, the lepton+jets events and the hadronic events. The different branching ratios of $t\bar{t}$ events, resulting from the combinations of the two W-boson decays, are presented in table 3. A good compromise of high statistic samples with a large background contamination and low statistic samples with low background contamination is the selection of lepton+jets events, where one top quark decays semileptonically and where the second top quark decays hadronically. The top quark events in the lepton plus jets channel are thus characterized by a well isolated high-momentum lepton and substantial missing energy due to undetected neutrino from the leptonic W decay, and a number of high-energy jets due to the hadronic W decay and by two b-jets originating each from a top quark decay. In figure 7 an event display of a $t\bar{t}$-event candidate is shown.

In order to select $t\bar{t}$-events only electrons and muons are considered as charged leptons, no taus, since the signature of taus in the detector is not as clear as of electrons or muons. Isolated electrons and muons with a transverse momentum p_T above 20 GeV are required. Isolated means, that in a certain cone around the charged lepton is almost no energy deposition from further particles in the calorimeter. To reduce background from Z-boson events only events with exactly one high-momentum lepton are accepted. A further reduction of Z-boson events is achieved, by removing events where the selected charged

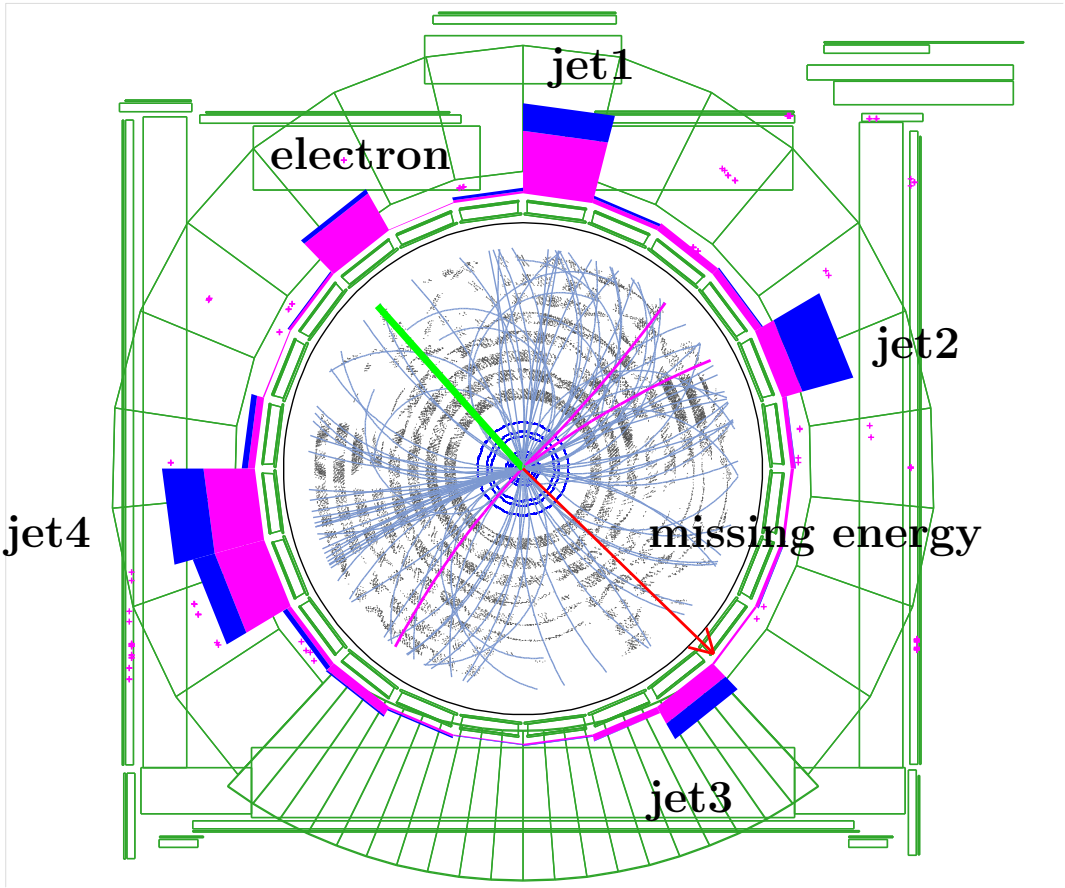

Abbildung 7: *Event display of a $t\bar{t}$ candidate with four jets. The energy of the electromagnetic calorimeter towers are drawn magenta, the energy of the hadronic calorimeter towers are drawn blue. The size of the cluster is proportional to the measured energy. The red arrow represents the direction of the missing energy. The inner part of the picture represents the tracking system. The gray points are hits in the COT, the blue points of the inner most rings are hits of the silicon vertex detector. The green line, an isolated track pointing to an energy deposition in the electromagnetic calorimeter represents the electron.*

lepton and a second object form an invariant mass within a window of the Z mass. Jets are reconstructed using the cone algorithm, where all particles within a cone of a given size are assigned to one jet. Jets are called high energetic jets, when the transverse energy is $E_T = \sqrt{p_T^2 + m_{jet}^2} > 15$ GeV and the absolute value of the pseudorapidity $\eta = 1/2 \cdot \ln((p+p_z)/(p-p_z)) = -\ln(\tan(\theta/2))$ is below 2.0. For the preselected sample used here in the Computer Praktikum at least one high energetic jet is required. Furthermore a missing transverse energy of ≥ 20 GeV is required.

One kind of background processes of $t\bar{t}$-events are W-boson plus jets production. Two different types of W-production can be distinguished. On the one hand the jets originating from light quarks, then one jet has to be misidentified as a b-jet (mistags). On the other hand one or more jets originate from a c- or b-quark (W + heavy flavor events). A further source of background events are QCD processes where one jet fakes an electron and another jet is misidentified as a b-quark jet (QCD background). The last very small contribution of background are di-boson and single top production (Electroweak backgrounds). $t\bar{t}$-events are characterized by a large partonic center of mass energy ($\sim$ invariant mass of the top pair) and thus also by a large transverse energy of the total event. For the production of background events not such a large partonic center of mass energy is necessary and thus a smaller transverse energy of the total event is expected. Therefore this quantity can be used to extract the $t\bar{t}$-signal. Since the shape of this variable is for the most background types very similar, only the W-boson plus light jet background is considered in the Computer Praktikum.

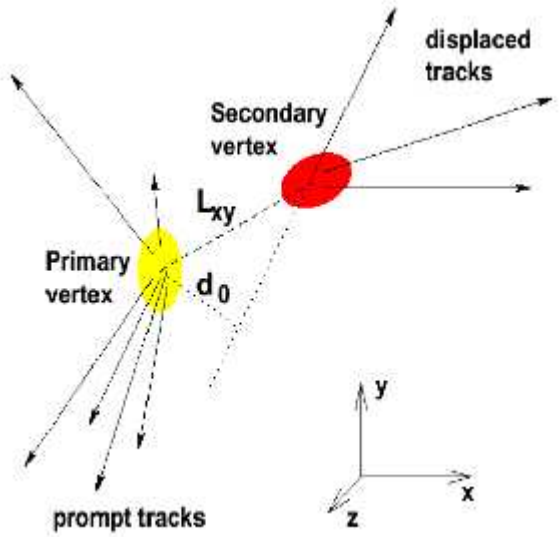

Abbildung 8: *General principle of b-tagging. The impact parameter d_0 and the decay length L_{xy} are sketched.*

In $t\bar{t}$ events two b-jets should exist. For the identification of b-jets, thus jets, which contain one or more B-hadrons, the long lifetime of the B hadrons is exploited. The travel

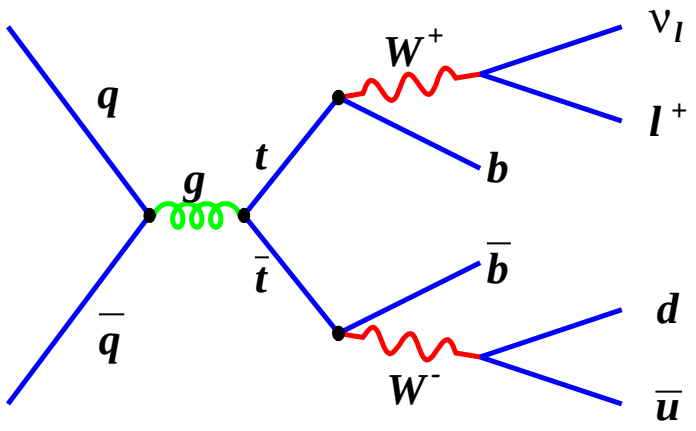

Abbildung 9: *Feynman diagram of the production and semi-leptonic decay of $t\bar{t}$-events.*

distance of a B hadron from its production vertex to its decay vertex is large enough to resolve it using the silicon trackers. b-jets coming from top quark decays at the Tevatron have an average p_T of about 65 GeV. The lifetime of a B hadron is thus, on average, 1.5 picoseconds in the lab frame. Therefore, the average distance traveled before decaying is approximately 7.5 millimeters. The b-tagging algorithm used by CDF, looks for tracks in each jet that are displaced from the primary vertex. The impact parameter has to be $|d_0| \leq 0.3$ cm (see figure 8). If there are at least two of these displaced tracks in the jet the tagging algorithm attempts to fit these tracks to a common vertex. As a final step the tagging algorithm computes the distance between the primary and secondary vertex in the $r - \phi$ plane, L_{xy} (fig. 8) . A cut on the significance L_{xy}/σ_{xy} of the displacement of ≥ 3 is required for so called b-tagged jets. Requiring that at least one selected jet is tagged as b-jet leads to a strong background reduction.

5 Full Reconstruction of $t\bar{t}$-events

In order to measure the mass of the top quark, the kinematics of the $t\bar{t}$ pair has to be reconstructed. For this purpose events with at least four high energetic jets, where one of those jets is b-tagged, are used in this Computer Praktikum. In such a sample the background from W plus jets events is small.

In figure 9 the Feynman diagram of the production and the semi-leptonic decay of $t\bar{t}$-events is illustrated. The reconstruction of the $t\bar{t}$ pair starts with the lepton, which can be reconstructed almost perfectly. As a second object the neutrino is reconstructed. Since the neutrino does not interact with the detector, it shows up only in the missing transverse energy ($\not\!\!E_T$). Unfortunately only the azimuthal angle and not the polar angle of the $\not\!\!E_T$ vector can be measured. Exploiting the fact, that the W-boson with a mass of $M_W = 80.42$ GeV decays into lepton and neutrino, a quadratic equation in the z-

component $P_{z,\nu}$ of the momentum of the neutrino is obtained:

$$P_{z,\nu}^2 - 2 \cdot \frac{\mu P_{z,l}}{\left(E_l^2 - P_{z,l}^2\right)} \cdot P_{z,\nu} + \frac{\left(E_l^2 P_{T,\nu}^2 - \mu^2\right)}{\left(E_l^2 - P_{z,l}^2\right)} = 0 \quad . \tag{1}$$

Here $P_{z,l}$ and E_l denote the z-component of the momentum and the energy of the electron or muon respectively. $P_{T,\nu}$ is the transverse momentum of the neutrino and is given by $\not\!\!E_T$. μ is defined as $M_W^2/2 + \cos(\Delta\Phi) P_{T,l} P_{T,\nu}$, where $\Delta\Phi$ is the azimuthal angle difference between the lepton and the $\not\!\!E_T$-vector. Since a quadratic equation leads in general to two solutions, the reconstruction procedure has to decide, which one has to be taken. If the solution is complex the real part is taken, otherwise the solution with the smaller value of $|P_{z,\nu}|$ is taken. That is reasonable, since the decay products of heavy particles like the W-boson are produced dominantly with a large transverse momentum and thus they are produced centrally in the detector. The selection of the solution with the smaller value of $|P_{z,\nu}|$ is in $\sim 78\%$ equal to the correct hypothesis.

The four-momentum of the leptonically decaying W-boson is then obtained by adding the four-momenta of the lepton and of the selected neutrino hypothesis. The next step is the reconstruction of the leptonically decaying top quark. All hypotheses obtained by adding the four-momentum of each selected high energetic jet and the four-momentum of the W-boson are considered. In total, the number of hypotheses is equal to the number of reconstructed jets N_{jets}. The four-momentum of the hadronically decaying W-boson is than obtained by combining the four-momenta of two of the selected jets, which are not assigned to the leptonically decaying top quark. This leads to $N_{jets} \cdot (N_{jets}-1) \cdot (N_{jets}-2)/2$ hypotheses. The last step is the assignment of a jet, not assigned so far to a light or b-jet from the leptonically decaying top quark, to the b-jet from the hadronic top decay. The four-momentum of this jet is than added to the four-momentum of the hadronically decaying W-boson resulting in the four-momentum of the hadronically decaying top quark. This leads to $N_{jets} \cdot (N_{jets}-1) \cdot (N_{jets}-2)/2 \cdot (N_{jets}-3)$ hypotheses for the jet assignment and thus for the full reconstruction of $t\bar{t}$-events due to the two solutions for the z-component of the neutrino momentum to $N_{jets} \cdot (N_{jets}-1) \cdot (N_{jets}-2) \cdot (N_{jets}-3)$ hypotheses. Furthermore the requirement, that the jets assigned to the light quarks are not b-tagged, is applied.

In order to choose the best event interpretation, a quantity χ^2, which gives a quantitative estimate how good the hypothesis matches the $t\bar{t}$ pair assumption, is calculated. Constraints on the mass of the hadronically decaying W-boson and the difference between both reconstructed top masses (two particles with the same mass) enter the calculation of χ^2. χ^2 is defined as:

$$\chi^2 \;=\; \frac{(m_{W\to jj} - M_{W\to jj,exp.})^2}{\sigma^2_{M_{W\to jj,exp.}}} + \frac{(m_{top\to bl\nu} - m_{top\to bjj})^2}{\sigma^2_{\Delta M_{t,exp.}}} \tag{2}$$

Here, $m_{W\to jj}$ is the reconstructed mass of the hadronically decaying W-boson and $m_{top\to bl\nu}$ and $m_{top\to bjj}$ are the reconstructed mass of the semileptonically decaying top

and the hadronically decaying top quark, respectively. The central value of the measured hadronically decaying W-mass $M_{W\to jj,exp.}$ and the width $\sigma_{M_{W\to jj,exp.}}$ of that distribution as well as of the distribution of the mass difference of the two top quarks $\Delta M_{t,exp.}$ are determined to be:

$$\begin{aligned} M_{W\to jj,exp.} &= 79.3\,\text{GeV} \\ \sigma_{M_{W\to jj,exp.}} &= 18.0\,\text{GeV} \\ \sigma_{\Delta M_{t,exp.}} &= 32.1\,\text{GeV} \end{aligned}$$